ELSEVIER

Ceramics International 25 (1999) 91–99

CERAMICS INTERNATIONAL

Electrical resistivity of porcelain in relation to constitution

S.P. Chaudhuri [a,*], P. Sarkar [a], A.K. Chakraborty [b]

[a] *Special Ceramics Section, Central Glass and Ceramic Research Institute, Calcutta-700032, India*
[b] *Instrumentation Section, Central Glass and Ceramic Research Institute, Calcutta-700032, India*

Received 20 June 1997; accepted 8 January 1998

Abstract

The electrical resistivity of porcelain samples has been measured from room temperature to 1200°C and it was found to depend on the concentration of the phases as well as the size and size-distribution of mullite crystals. The resistivity of porcelain was found to decrease with increase in amount, size and asymmetry of size-distribution of mullite crystals but increase with increase in quartz, cristobalite and glass content. Irrespective of constitution, resistivity of porcelain decreased with rise in temperature from about 10^{13} ohm-cm at room temperature to about 10^4 ohm-cm at 1200°C. The change in electrical resistivity of porcelain was primarily controlled by the defect structure of mullite and the composition and viscosity of the glassy phase.

Keywords: C. electrical conductivity; D. mullite; D. porcelain

1. Introduction

Porcelain consists of a glassy phase (matrix) and some crystalline phases which are dispersed/embedded in it. Mullite and quartz are very frequently found In the porcelain body [1]. Cristobalite is also detected in porcelain which had been subjected to prolonged heating [2]. Concentrations of phases changed as well as new phases appeared due to longtime use of porcelain body at elevated temperature [2]. Apart from this, significant variations in size, shape and distribution of the phases in porcelain resulted during continuous high temperature applications [3].

Porcelain is basically an insulator and its electrical resistivity at room temperature is about 10^{14} ohm-cm [4] but it drops with the rise in temperature. Each phase in the porcelain body has its specific influence on the resistivity shown by the body depending on its concentration and microstructural attributes. Temperature also plays an important role to control the nature of certain phases [5]. Structural characteristics of some of the phases are also responsible for change in the resistivity of porcelain body [6].

The phase composition including the phase concentration and the microstructure of porcelain can be changed by incorporating different mineralizers in the body [7,8]. Besides, a novel method to bring about such change in composition, concentration and microstructure of the phases in porcelain is the heat-treatment of the body under certain controlled conditions to recrystallise its glassy phase.

The rise in temperature of the porcelain body which is used as insulator may damage its insulation property due to decrease in Its resistivity. On the contrary, the porcelain body may be employed as conductor at higher temperature for the same reason, i.e., drop in its electrical resistivity with temperature. Application of porcelain as insulator is well-known but only a few reports [9–11] on the use of porcelain as ceramic heaters, heating elements, semiconducting material, etc., are available in the literature.

Investigations on the influence of constitution of porcelain on its electrical property are only a few. In the present study it is, therefore, attempted to correlate the electrical resistivity of porcelain, measured from room temperature to near maturing temperature, with the concentration of phases and also the size and size-distribution of the major crystalline phase (mullite) in it. The effect of temperature and heat-treatment (for recrystallisation of the glassy phase) on the electrical resistivity of porcelain has also been assessed.

* Corresponding author.

0272-8842/98/$—see front matter
PII: S0272-8842(98)00006-6

2. Experimental procedure

2.1. Sample preparation

A good quality china clay, a pottery grade quartz and a potash feldspar were used as the raw materials, The analytical reagent grade oxides of Fe, Ti, Cr, V and Nb were employed as mineralizers. Clay, quartz and feldspar were taken in the proportions of 63:12:25 wt% in the base composition and the oxides were incorporated in this composition individually or in combination to the extent of 2–8 wt%. In this way nine compositions were prepared. The ingredients were thoroughly wet mixed in pot mill to form the slip which was thereafter cast into plaster of Paris mould. The sample in disc shape having 25 mm dia and 5 mm thickness were dried and then fired at 14000°C for 1 h in an electric furnace and cooled overnight.

The discs of each of nine compositions were divided into two halves. One half was retained (for before heat-treatment sample) and the other half was heat-treated (for after heat-treatment samples) at 1150°C for 50 h in an electric furnace and then cooled overnight, The preparation and heat-treatment of the samples (compositions) were elaborated in an earlier paper [2].

2.2. Constitution

The phase assemblage and the concentrations of phases in the samples both before heat-treatment and after heat-treatment were determined by X-ray diffractometry and reported in details elsewhere [2]. Mullite, quartz and glass were found in the samples without heat-treatment but an additional phase, i.e., cristobalite was detected in the heat-treated samples.

The size, size-distribution and the shape, i.e., aspect ratio of mullite, the major crystalline phase, in the samples with and without heat-treatment were determined by X-ray diffraction, transmission electron microscopy and statistical analysis. The detailed study was included in another paper [3]. The heat-treatment caused increase of crystal size and aspect ratio but made the size-distribution more symmetric.

2.3. Measurement of electrical resistivity

The ground and polished discs of about 20 mm diameter and 3 mm thickness were coated with a platinum paste on both sides. These were dried and fired at 1000°C for 15 min to deposit metallic platinum on the surface.

2.3.1. At room temperature

The instrumental set up is shown by the block diagram (Fig. 1). The platinum coated disc was enclosed in a teflon holder and then placed inside a properly shielded

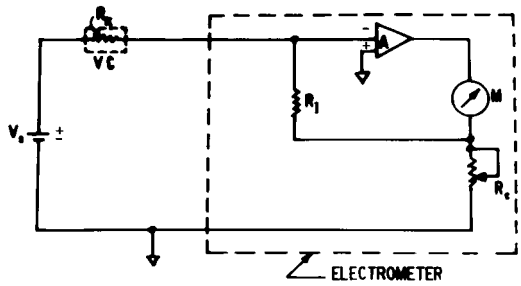

V_s - CONSTANT D.C. VOLTAGE SOURCE
R_x - UNKNOWN RESISTANCE (SAMPLE RESISTANCE)
VC - VACUUM CHAMBER CARRYING SAMPLE IN TEFLON HOLDER
R_1 - KNOWN INPUT RESISTANCE SUPPLIED BY ELECTROMETER
A - AMPLIFIER (BUILT INSIDE ELECTROMETER)
M - ANALOGUE TYPE METER INSIDE ELECTROMETER TO READ CURRENT/VOLTAGE
R_c - CALIBRATING RESISTANCE (BUILT INSIDE ELECTROMETER)

Fig. 1. Instrumental set up for electrical resistivity measurement at room temperature.

vacuum chamber (10^{-2} mbar). The electrometer provided a high input resistance (R_1) in series and a constant DC voltage (V) of about 1.5 volts was applied to the sample from a battery. The electrometer measured the voltage (V_1) across the input resistance and the current (I) flowing through the circuit. The sample resistance (R) was, therefore

$$R = V/I \tag{1}$$

and its resistivity (ρ) was

$$\rho = R(A/l) \tag{2}$$

where A and l were area and thickness of the sample.

2.3.2. At higher temperature

The platinum coated surfaces of the disc were spot-welded with platinum lead wires and suspended inside an electrically heated furnace. The lead wires were connected to a device that measured the sample resistance. A constant voltage was supplied to the sample and the output voltage proportional to sample resistance was given by the high impedance amplifier. This output voltage was fed to the digital panel meter (DPM) amplifier and also the X-T recorder amplifier. Fig. 2 is a schematic diagram of the instrumental assembly.

The sample resistance was directly read from the DPM but continuously recorded on the stripchart recorder with temperature. Calibration curves, i.e., pen displacement vs standard resistance, were drawn and the resistance of the sample was computed from the

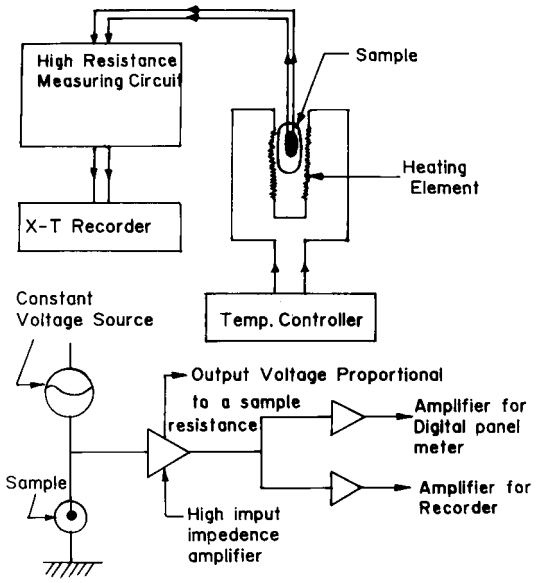

Fig. 2. Instrumental set up for electrical resistivity measurement upto high temperature.

curves by knowing the pen displacement at any temperature. The resistivity of the sample was calculated as done before.

2.4. Determination of band gap energy

The electrical resistivity (ρ) of the sample is related to temperature by the equation

$$\rho = \rho_0 \exp(E/2KT) \quad (3)$$

where ρ and ρ_0 are resistivities at any temperature and 0° respectively. E, K, T denote activation energy, Boltzmann constant (8.62×10^{-5} eV) and absolute temperature, respectively.

The activation energy of electrical resistivity for each sample was calculated from the slope of $\log_{10}\rho - 1/T$ plot (R.T.–1200°C) as follows:

$$E = \text{slope} \times 4.606 \times 8.62 \times 10^{-5} \text{ eV} \quad (4)$$

which is also the band gap energy (Eg).

3. Results

The electrical resistivity ($\log_{10}\rho$) of the samples before and after heat-treatment measured from room temperature to 1200°C have been included in Tables 1 and 2, respectively. As shown, the resistivity of the samples decreased with rise in temperature and dropped to 10^5–10^4 ohm-cm order at 1200°C. In almost all cases the resistivity at any temperature of a composition after heat-treatment was less than that before heat-treatment,

Table 1
Electrical resistivity ($\log_{10}\rho$) of the samples before heat-treatment

Temperature (°C)	$\text{Log}_{10}\rho$ (ohm-cm) of the samples								
	1B	2B	3B	4B	5B	6B	7B	8B	9B
26	14.13	13.94	13.68	13.79	14.02	13.79	14.04	14.44	14.33
100	–	–	–	–	–	–	–	–	–
200	–	–	–	–	–	–	–	–	–
300	7.69	8.42	8.42	8.65	8.90	8.50	8.58	8.51	8.39
400	7.67	8.68	7.81	8.10	8.49	7.84	8.16	7.39	17.50
500	7.89	7.05	7.44	7.65	7.52	7.35	7.43	6.85	7.35
600	7.24	7.68	7.02	7.08	7.44	6.92	7.07	6.20	7.36
700	6.48	6.29	6.05	6.48	6.90	6.22	6.62	5.93	7.20
800	6.02	5.91	5.33	6.20	6.47	5.77	6.28	5.98	6.67
900	5.70	5.68	5.02	6.09	6.17	5.53	5.86	5.81	6.35
1000	5.67	5.66	4.78	5.88	5.99	5.45	5.62	5.73	6.08
1100	5.51	5.44	4.72	5.60	5.73	5.22	5.27	5.46	5.73
1200	5.25	5.18	4.55	5.22	5.34	4.83	5.02	5.26	5.22

Table 2
Electrical resistivity ($\log_{10}\rho$) of the samples after heat-treatment

Temperature (°C)	$\text{Log}_{10}\rho$ (ohm-cm) of the samples								
	1A	2A	3A	4A	5A	6A	7A	8A	9A
26	13.95	13.90	13.53	13.74	13.71	13.81	13.73	13.99	13.96
100	–	–	–	–	–	–	–	–	–
200	–	–	–	–	–	–	–	–	–
300	8.20	8.13	8.13	8.11	8.19	8.28	8.12	8.04	8.16
400	7.44	7.28	6.64	7.37	7.26	7.82	7.44	7.07	7.38
500	6.64	7.31	6.16	6.86	6.29	7.17	7.13	6.26	6.82
600	5.99	6.80	5.74	6.54	6.70	6.64	7.02	5.76	7.00
700	6.37	6.36	5.54	6.08	6.20	6.10	6.65	5.68	6.64
800	6.00	6.11	5.89	5.71	5.88	5.82	6.35	5.54	6.13
900	5.75	5.99	5.56	5.72	5.48	5.60	6.35	5.39	5.87
1000	5.62	5.85	4.82	5.56	5.31	5.46	6.20	5.27	5.52
1100	5.44	5.56	4.43	5.30	5.08	5.33	5.72	5.07	5.27
1200	5.12	5.28	4.01	4.95	4.84	4.72	5.26	4.95	4.78

it is worth mentioning that the resistivity of heat-treated samples reached the 10^6 ohm-cm order (semiconductor resistivity zone) at 530–815°C whereas the resistivity of unheat-treated samples entered this zone at 640–1000°C.

The resistivity of all the samples at room temperature, 1000 and 1200°C along with their constitutional parameters are given in Table 3.

The dependence of resistivity of the samples, both before and after heat-treatment, on their constitutional parameters is exhibited in Figs. 3–8. The salient features of the relationships are mentioned in the following paragraphs.

The resistivity of the heat-treated and unheat-treated samples decreased with increase in their mullite content (Fig. 3). Minimum resistivity was attained at 7.5 wt% quartz content for before heat-treatment samples and 5.5 wt% quartz content for after heat-treatment samples (Fig. 4). The after heat-treatment samples had minimum

Table 3
Electrical resistivity ($\log_{10}\rho$) of the samples and their constitutional parameters

Sample no.	$\text{Log}_{10}\rho$ (ohm-cm) at			Constitutional parameters					
	Room temperature	1000°C	1200°C	Mullite (wt%)	Quartz (wt%)	Cristobalite (wt%)	Glass (wt%)	Size of mullite (micron)	Skewness
1B	14.13	5.67	5.25	32.7	4.5	0.2	62.6	0.1364	0.5701
2B	13.94	5.66	5.18	28·5	6.5	0.0	65.0	0.1460	0.5549
3B	13.68	4.78	4.55	39.7	7.5	0.3	52.5	0.2428	0.5270
4B	13.79	5.88	5.22	33.5	10.7	0.0	55.7	0.1258	0.6110
5B	14.02	5.99	5.34	35.5	3.0	0.0	63.5	0.1790	0.3952
6B	13.79	5.45	4.83	36.0	8.3	0.4	55.4	0.1298	0.4985
7B	14.04	5.62	5.02	32.7	6.3	0.3	60.7	0.1233	0.5561
8B	14.44	5.73	5.26	29.7	5.5	0.4	64.3	0.1306	0.6176
9B	14.33	6.08	5.22	43.0	9.7	24.8	22.4	0.2084	0.4182
1A	13.95	5.62	5.12	41.5	5.4	22.8	30.4	0.1443	0.5484
2A	13.90	5.85	5.28	35.5	3.7	27.8	33.0	0.1791	0.3213
3A	13.53	4.82	4.01	43.0	5.7	28.6	22.6	0.3228	0.7296
4A	13.74	5.56	4.95	41.5	6.2	25.2	27.2	0.1772	0.4165
5A	13.71	5.31	4.84	40.7	5.3	31.0	23.0	0.4473	0.6506
6A	13.81	5.46	4.72	43.0	5.6	25.6	25.8	0.2086	0.3799
7A	13.73	6.20	5.26	43.0	5.7	27.0	24.3	0.1500	0.2433
8A	13.99	5.27	4.95	43.0	5.0	24.4	27.6	0.1411	0.2766
9A	13.96	5.52	4.78	42·3	5.0	29.0	23.7	0.2550	0.4220

B, before heat-treatment; A, after heat-treatment.

resistivity at 29 wt% cristobalite content (Fig. 5). The resistivity of both the heat-treated and unheat-treated samples increased with the rise in their glassy phase content (Fig. 6).

As the size of mullite crystals increased from 0.14 μ to about 0.30 μ, the resistivity of before heat-treatment and after heat-treatment samples decreased. However, slight increase in resistivity was noticed between 0.12 and 0.14 μ size for unheat-treated samples and beyond 0.30 μ, size for heat-treated samples (Fig. 7).

The resistivity decreased steadily with the rise in skewness and reached minimum at a skewness 0.5 for before heat-treatment samples and a skewness 0.4 for after heat-treatment samples. Further increase in skewness upto 0.6 caused increase in resistivity (Fig. 8).

The Arrhenius plots of a few representative samples are displayed in Fig. 9. The values of band gap energy (Eg) calculated from such plots are presented in Table 4. It was observed that Eg varied from 1.08 to 1.33 eV and heat-treatment resulted in reduction of Eg. The Eg values of samples along with their parameters of constitution are shown in Table 5.

The relationships between Eg and concentration of mullite in the samples (B) before heat-treatment and (A) after heat-treatment are demonstrated in Fig. 10. Although the nature of the curves marked (B) and (A) was different, it was revealed that the Eg of two categories of samples decreased with the increase in their mullite content. It is noteworthy that curve (B) was concave and curve (A) was convex, meeting together at a point where two samples, one from before heat-treatment (B) and one from after heat-treatment (A), coexist.

4. Discussion

The porcelain body is composed of phases such as mullite, quartz, cristobalite and glass. Its electrical resistivity is dependent on the resistivity of each of these phases, both at room and at elevated temperatures. Besides, microstructural characteristics, such as crystal size and size-distribution also contribute to the electrical resistivity of the body because they influence the passage of current through the body.

Mullite crystal has inherent defect centres as 0^{2-} ion vacancy [12] in its structure and it is a potential ionic conductor [13]. Substitution of Al^{3+} ion in the (AlO_6)octahedral and (AlO_4)tetrahedral sites of mullite lattice by the transition metal ions, M^{n+} can make it *n*-type (if $n > 3$) and *p*-type (if $n < 3$) electronic conductor. Apart from this, substitution of Al^{3+} ion by M^{n+} ion (if $n = 3$) in the octahedral or tetrahedral position and only incorporation of M^{n+} ion in the interstitials or structural channels of mullite lattice can impart electrical conductivity in mullite [14,15]. Under these circumstances resistivity of mullite decreased by several orders of magnitude at elevated temperature [25].

Quartz and cristobalite have high electrical resistivity at room temperature [16]. With the rise in temperature resistivity does decrease noticeably.

The glassy phase is derived from the feldspar (potash) component in the porcelain composition. The PCE of the K-feldspar is 8–10 (1225–1260°C) [17,18]. It starts softening at about 1225°C and at this temperature the viscosity of the glassy phase in these porcelain

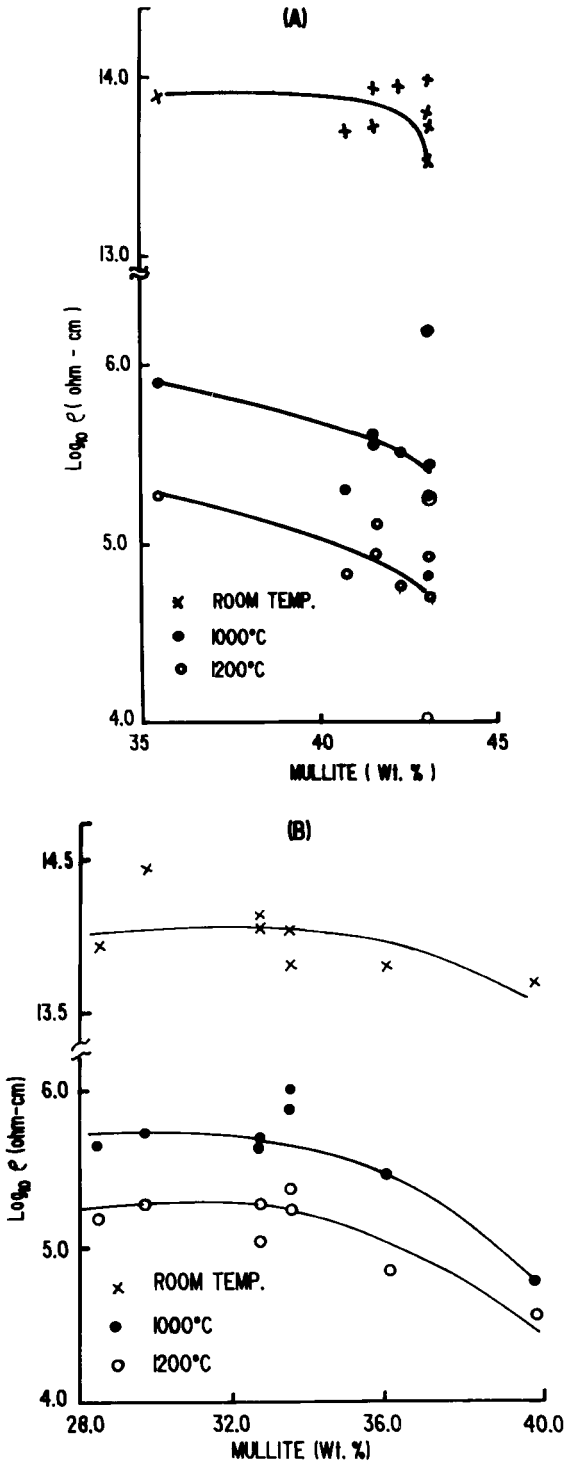

Fig. 3. Dependance of electrical resistivity of porcelain on the concentration of mullite; (B) sample before heat-treatment, (A) sample after heat-treatment.

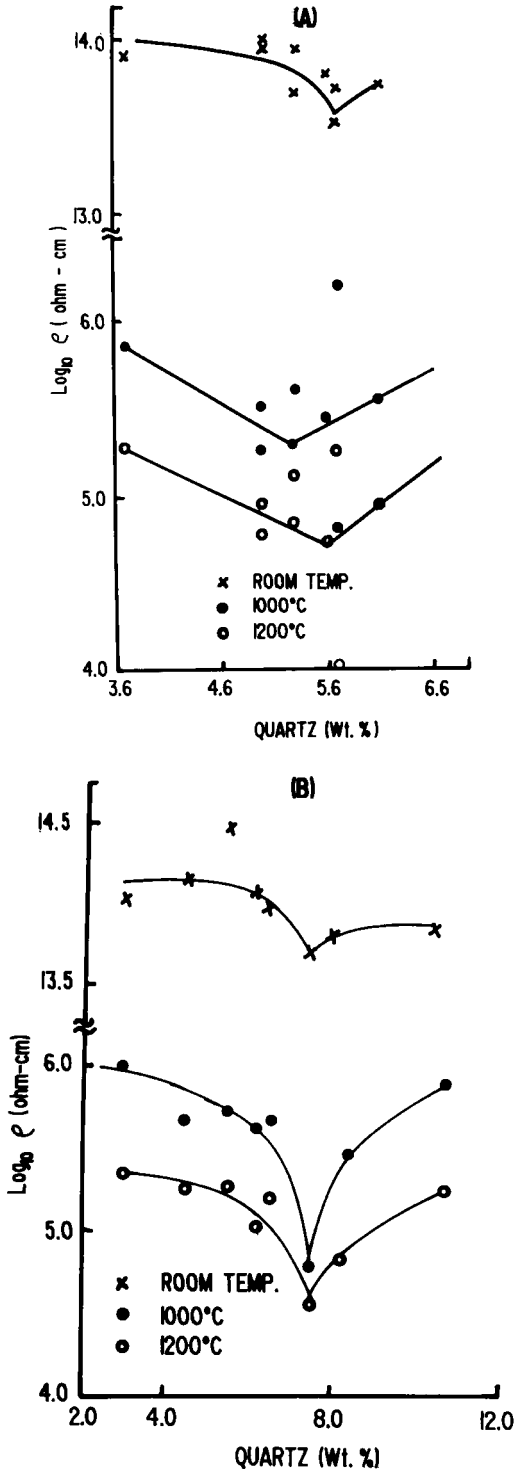

Fig. 4. Dependance of electrical resistivity of porcelain on the concentration of quartz; (B) sample before heat-treatment, (A) simple after heat-treatment.

compositions was found to be greater than 10^{11} poise [19,20]. At a temperature employed for the measurement of resistivity, such as 1200°C (maximum in this study), therefore, the ions in the feldspathic glass of porcelain are held together by moderately strong bonds and the movement of the alkali ions (K^+, Na^+) in the applied electric field became restricted. Consequently, the electrical resistivity of glass in porcelain was high.

In the polycrystalline material the grains/crystals create boundaries between them which have significant

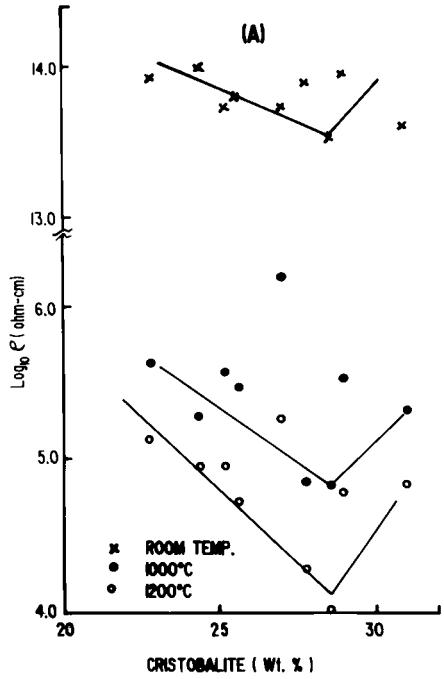

Fig. 5. Dependance of electrical resistivity of porcelain on the concentration of cristobalite; (A) sample after heat-treatment.

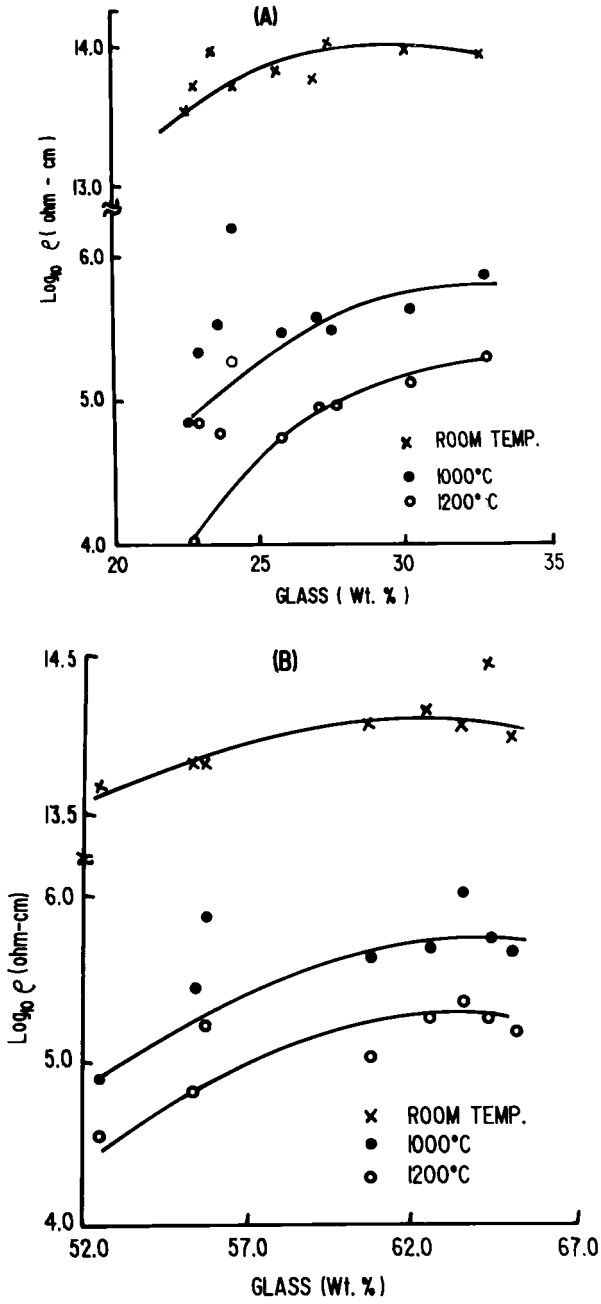

Fig. 6. Dependance of electrical resistivity of porcelain on the concentration of glassy phase; (B) sample before heat-treatment, (A) sample after heat-treatment.

control over the flow of current through the material because the boundaries determine the mean free path for electrical conductivity of the material. As the grain boundaries decrease in number but increase in size, the length of the mean free path increases. Thus, the electrical conductivity of the material improves.

The skewness is a measure of asymmetry of size distribution of crystals and, therefore, the compactness of their arrangement. A more compact arrangement of crystals with defect structure (and semiconducting nature) in a body offers a continuous path for flow of current and thereby lowers its resistivity.

The observed changes in the electrical resistivity of porcelain body in relation to individual parameter can, therefore, be explained by the specific role played by each parameter as described above.

The decrease in resistivity of porcelain bodies with the increase in their mullite content (Fig. 3) was the consequence of the semiconducting nature of mullite crystals that arises from its defect structure and incorporation of M^{n+} ions in its lattice. The high resistivity of the glassy phase in the porcelain body was responsible for increase of resistivity of the bodies with the increase in the concentration of their glassy phase (Fig. 6). Both quartz and cristobalite are phases of high electrical resistivity and, therefore, increase in their concentration in porcelain body caused rise in its resistivity. The rise was observed from 7.5 wt% quartz in the samples before heat-treatment but from 5.5 wt% quartz in the sample after heat-treatment (Fig. 4). The low concentration of quartz in the latter samples was due to the parallel effect of cristobalite that was generated in them. The initial drop in resistivity may be attributed to the strong influence of mullite which outweighed the effect of quartz and cristobalite.

That the resistivity of a porcelain composition, at any temperature after heat-treatment was less than that before heat-treatment (Tables 1 and 2) may be explained by the predominating effect of mullite. The

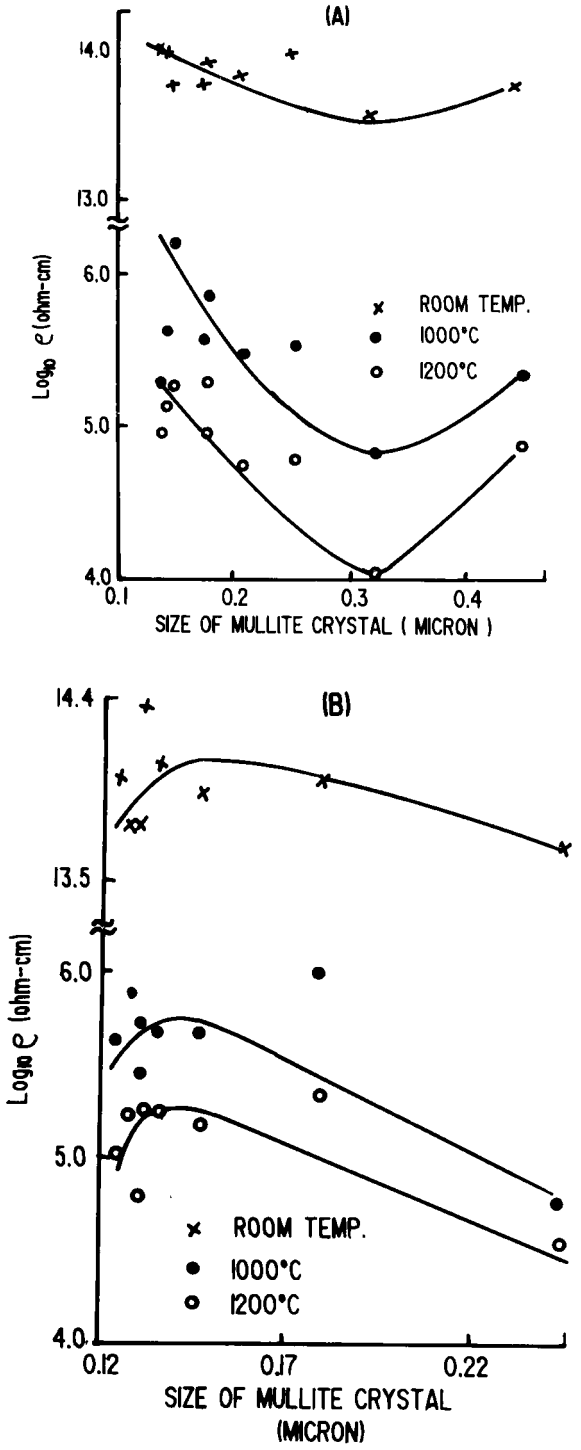

Fig. 7. Dependance of electrical resistivity of porcelain on the size of mullite crystals; (B) samples before heat-treatment. (A) samples after heat-treatment.

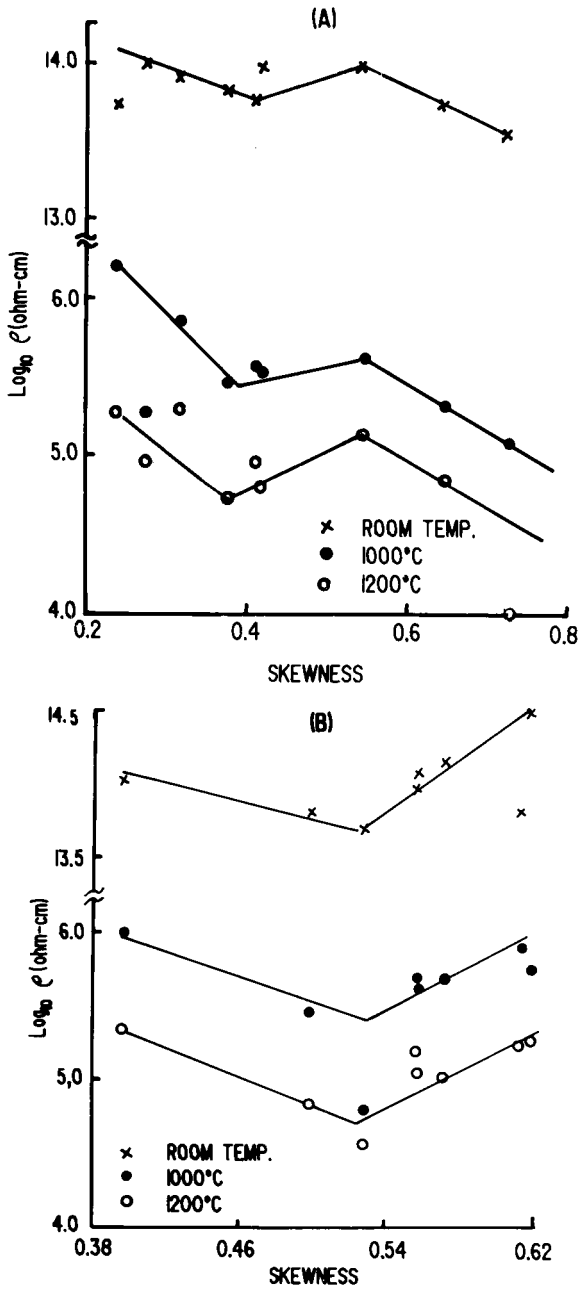

Fig. 8. Dependance of electrical resistivity of porcelain on the asymmetry of size-distribution (skewness) of mullite crystals; (B) sample before heat-treatment, (A) sample after heat-treatment.

higher concentration of mullite in the heat-treated samples more than counterbalanced the combined effect of cristobalite and glass.

The increase in the size of mullite crystals/grains from $0.14\,\mu$ to $0.30\,\mu$ resulted in decrease of the number of boundaries between them but increase in boundary size. Therefore, the resistivity of a porcelain body decreased with increase in mullite crystal size (Fig. 7). The decrease in resistivity of porcelain body with the increase in skewness (asymmetry of size-distribution) upto 0.5 and 0.49 respectively, for unheat-treated and heat-treated samples (Fig. 8) was ascribed to better compactness of juxtaposed mullite crystals with higher skewness leading to higher conductivity.

The Eg value decreased with increase in mullite content of both heat-treated and unheat-treated samples

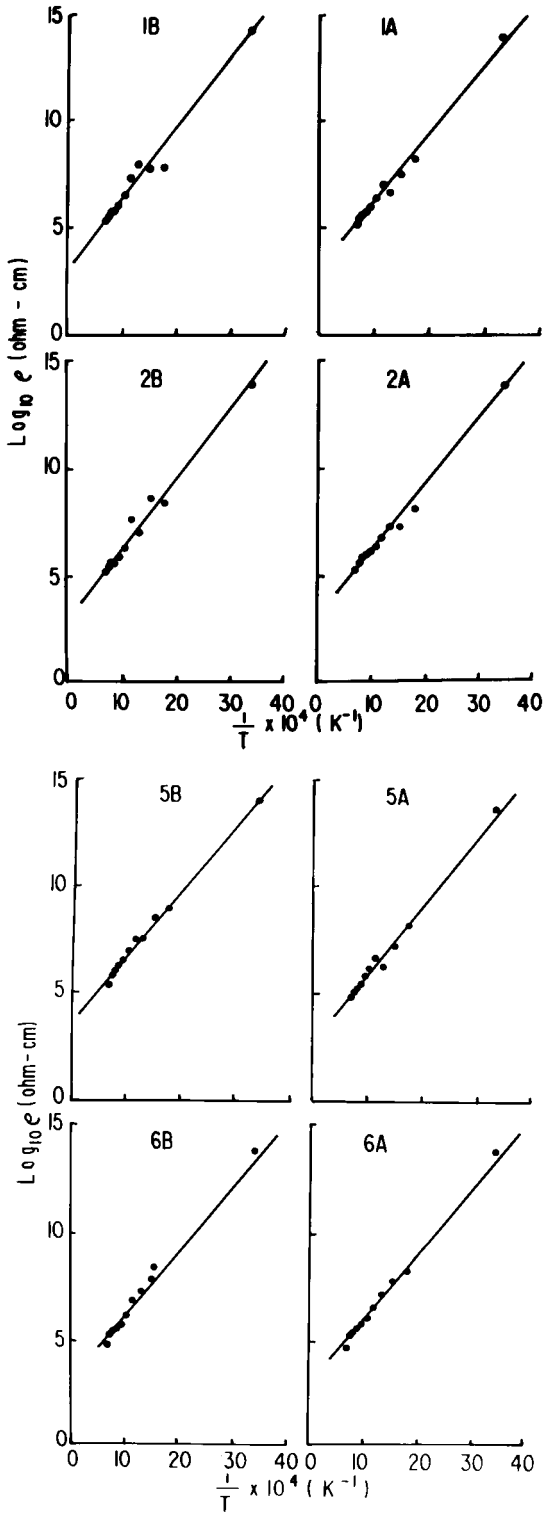

Fig. 9. Arrhenius Plots ($\log_{10}\rho$-$1/_T$) of representative porcelain samples: (B) sample before heat-treatment; (A) sample after heat-treatment.

(Fig. 10). The nature of the curves representing the two categories of samples is significantly different because their phase assemblages varied widely [2]. However the decreasing trend of curves B and A in Fig. 10 with the rise in the concentration of mullite showed that mullite had been the most active phase to lower Eg of the samples. This was supported by the results recorded in Table 5. The Eg of a heat-treated sample containing higher amount of mullite and cristobalite was less than that of the corresponding unheat-treated sample containing only mullite (almost no cristobalite). So, the effect of mullite dominated. On the other hand, off the two samples having the same mullite content, the Eg of the heat-treated one was higher than the Eg of the unheat-treated one (Fig. 10). This was due to the reverse effect of cristobalite.

The phase assemblages of the samples containing Nb_2O_5 before and after heat-treatment were almost identical (Table 5). A virtually stable phase composition

Table 4
Eg values of samples

Sample no.	Composition	Eg (eV)	
		Before heat-treatment (B)	After heat-treatment (A)
1.	Base composition (B.C.)	1.33	1.24
2.	B.C. + 8% TiO_2	1.32	1.28
3.	B.C. + 3% V_2O_5	1.31	1.27
4.	B.C. + 2.6% Fe_2O_3	1.22	1.09
5.	B.C. + 2.6% TiO_2	1.26	1.25
6.	B.C. + (1.5%V_2O_5 + 1.3%Fe_2O_3)	1.21	1.21
7	B.C + (1.5%V_2O_5 + 1.3%TiO_2)	1.31	1.08
8.	B.C. + 2.5% Cr_2O_3	1.27	1.20
9.	B.C. + 2% Nb_2O_5	1.20	1.23

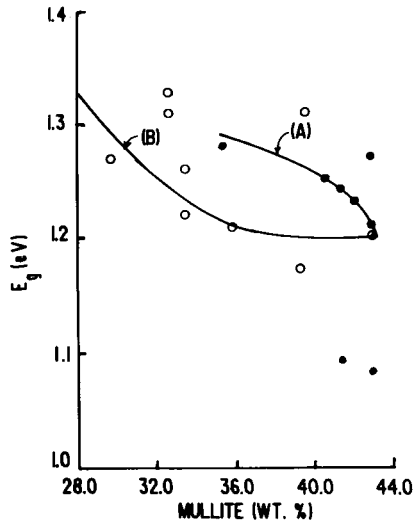

Fig. 10. Relationship between band gap energy (Eg) of porcelain and concentration of mullite; (B) sample before heat-treatment; (A) sample after heat-treatment.

Table 5
Eg values of samples and their constitutional parameter

Sample no.	Eg (eV)	Constitutional parameters					
		Mullite (wt%)	Quartz (wt%)	Cristobalite (wt%)	Glass (wt%)	Size of mullite (micron)	Skewness
1B	1.33	32.7	4.5	0.2	62.6	0.1364	0.5701
2B	1.32	28.5	6.5	0.0	65.0	0.1460	0.5549
3B	1.31	39.7	7.5	0.3	52.5	0.2428	0.5270
4B	1.22	33.5	10.7	0.0	55.7	0.1258	0.6110
5B	1.26	33.5	3.0	0.0	63.5	0.1790	0.3962
6B	1.21	36.0	8.3	0.4	55.4	0.1298	0.4985
7B	1.31	32.7	6.3	0.3	60.7	0.1233	0.5561
8B	1.27	29.7	5.5	0.4	64.3	0.1306	0.6176
9B	1.20	43.0	9.7	24.8	22.4	0.2084	0.4182
1A	1.24	41.5	5.4	22.8	30.4	0.1443	0.5484
2A	1.28	35.5	3.7	27.8	33.0	0.1791	0.3213
3A	1.27	43.0	5.7	28.6	22.6	0.3228	0.7296
4A	1.09	41.5	6.2	25.2	27.2	0.1772	0.4165
5A	1.25	40.7	5.3	31.0	23.0	0.4473	0.6506
6A	1.21	43.0	5.6	25.6	25.8	0.2086	0.3799
7A	1.08	43.0	5.7	27.0	24.3	0.1500	0.2433
8A	1.20	43.0	5.0	24.4	27.6	0.1411	0.2766
9A	1.23	43.23	5.0	29.0	23.7	0.2550	0.4220

B, before heat-treatment; A, after heat-treatment.

was reached in these two samples and, therefore, the Eg values of these two samples, before and after heat-treatment, happened to be the same (Fig. 10).

Among the metal oxides added to the porcelain compositions, V_2O_5 was found to be the most efficient and caused maximum lowering of resistivity of the composition. Most possibly it was due to the V^{5+} ion which has high charge (5+), small size (0.54 Å) and moderate mobility. The V_2O_5 is also a good flux and reduced glass viscosity considerably and much more than the reduction of glass viscosity effected by Cr_2O_3, TiO_2, etc. [21] The movement of the V^{5+} ion through the glassy phase of very low viscosity in this composition with V_2O_5 became much easier than that of Cr^{3+}, Ti^{4+}, etc., ions through high viscosity glassy phase in the compositions with Cr_2O_3, TiO_2, etc. The ionic conductivity of the porcelain composition containing V_2O_5 was enhanced due to faster transport of the current carrier V^{5+} ion through this composition.

5. Conclusions

The electrical resistivity of porcelain decreased with the rise in temperature, i.e., from 10^{13} ohm-cm at room temperature to 10^4 ohm-cm at 1200°C.

The phase composition and microstructure of porcelain controlled its electrical resistivity, i.e., increase in concentration, size and skewness of size-distribution of mullite crystals lowered the resistivity but increase in concentration of quartz, cristobalite and glass raised the resistivity.

The cations of the metal oxide (mineralizers) added to the porcelain compositions impart some ionic conductivity to them. V^{5+} ion of V_2O_5 appeared to be the most efficient in this respect.

The band gap energy (Eg) of porcelain varied from 1.08 to 1.33 eV, i.e., well within that found for semiconductors [22]. Porcelains, therefore, work like semiconductors, of course, above room temperature.

Acknowledgement

One of the authors, P. Sarkar, is grateful to the Council of Scientific and Industrial Research, India for granting a research fellowship to him to carry out this study.

References

[1] K.H. Schüller, Trans. Brit. Ceram. Soc. 63 (1964) 103.
[2] S.P. Chaudhuri, P. Sarkar, J. Eur. Ceram. Soc. 15 (1995) 1031.
[3] S.P. Chaudhuri, P. Sarkar, J. Eur. Ceram. Soc. 16 (1996) 851.
[4] R.C. Buchanan, Properties of ceramic insulators, in: R.C. Buchanan (Ed.), Ceramic Materials for Electronics, Marcel Dekker, New York, 1986, pp. 1–71.
[5] S.P. Chaudhuri, S.K. Patra, A.K. Chakraborty, J. Mater. Sci., submitted.
[6] S.P. Chaudhuri, S. Bandyopapdhyay, N. Mitra, Interceram 44 (1995) 300.
[7] S.P. Chaudhuri, Am. Ceram. Sec. Bull. 53 (1974) 169.
[8] S.P. Chaudhuri, Am. Ceram. Soc. Bull. 53 (1974) 251.
[9] M. Kumagai, K. Kato, H. Takeuti, et al., US5,006,957, 9 April 1991; Ceram. Abst. 70-10803 P (1991).
[10] T. Wang, US D304,230, 24 Oct., 1989; Ceram. Abstr., 69–06 446 P (1990).
[11] H. Baudry, M. Moneraye, C. Morhaim, US 4,973,826, 27 November 1990; Ceram. Abstr., 70-05595 P (1991).
[12] H.W. Taylor, J. Soc. Glass Technol. 16 (1932) 111 T.
[13] G.-Y. Meng, R.A. Huggins, Mater. Res. Bull. 18 (1983) 581.
[14] S.P. Chaudhuri, S.K. Patra, J. Am. Ceram. Soc., submitted.
[15] D. Sanyal, S.K. Patra, S.P. Chaudhuri, B.N. Ganguli, D. Banerjee, U. De, R.L. Bhattacharya, J. Mater. Sci. 31 (1996) 3447.
[16] J.F. Shackelford, W. Alexander, J.S. Park (Eds.), Materials Science and Engineering Handbook, CRC Press, Bocan Raton, FL, 1994, pp. S395–401.
[17] L.P. William, Ceramics, Reinhold, New York, 1961.
[18] F. Singer, S.S. Singer, Industrial Ceramics, Chapman and Hall, London, 1963, pp. 395–399.
[19] S.P. Chaudhuri, Trans. Ind. Ceram. Soc. 32 (1973) 70.
[20] P.P. Budnikov, The Technology of Ceramics and Refractories, Edward Arnold, London, 1964, pp. 500–570.
[21] J. Williamson, Miner. Mag. 37(291) (1970) 759.
[22] L.H. Van Vlack, A Text Book of Materials Technology, Addison–Wesley, Reading, MA, 1973, pp. 270–292.